

Pt/Ti/SiO₂/Si substrates

G. R. Fox,^{a)} S. Trolier-McKinstry, and S. B. Krupanidhi

Materials Research Laboratory, The Pennsylvania State University, University Park, Pennsylvania 16802

L. M. Casas

*Army Research Laboratory, Electronic and Power Sources Directorate, AMSRL-EP-EC-M,
Fort Monmouth, New Jersey 07703-5601*

(Received 6 April 1994; accepted 3 March 1995)

Pt/Ti/SiO₂/Si structures have been studied to investigate the structural, chemical, and microstructural changes that occur during annealing. Grain growth of the as-deposited Pt columns was observed after annealing at 650 °C, and extensive changes in the Pt microstructure were apparent following a 750 °C anneal for 20 min. In addition, two types of defects were identified on the surfaces of annealed substrates. Defect formation was retarded when the surface was covered with a ferroelectric film. Concurrent with the annealing-induced Pt microstructure changes, Ti from the adhesion layer between the Pt and the SiO₂ migrated into the Pt layer and oxidized. It was shown with spectroscopic ellipsometry and Auger electron spectroscopy that for long annealing times, the titanium oxide layer can reach the Pt surface. Consequently, at the processing temperatures utilized in preparing many ferroelectric thin films, the substrate is not completely inert or immobile. The changes associated with Ti migration could be especially problematic in techniques that require the substrate to be heated prior to film deposition.

I. INTRODUCTION

The development of ferroelectric devices that are integrated with Si based technology has produced a need for electrode materials that also act as reaction barrier layers during the processing of the ferroelectric material. This need for electrically conductive barrier layers is particularly evident in the systems that employ Pb-based perovskites since processes that form a fully crystallized ferroelectric phase require temperatures above 500 °C, and PbO and Si react at temperatures as low as 500 °C to form lead silicate phases.¹⁻⁴ Not only do the PbO and Si react to form a lead silicate phase, but pores are also formed at the film/substrate interface, which causes deformation of the film surface and an increase in the surface roughness. This type of reaction leaches Pb from the ferroelectric and will severely degrade the observed electrical properties.

While Pt does not react with Pb-based perovskites over the temperature range of interest for the processing of ferroelectric films, it cannot be used directly on Si as a barrier layer electrode because of its own reactivity with Si at temperatures as low as 400 °C.^{5,6} The resultant diffusion of Si into the Pt to form a platinum silicide causes a loss in the integrity of the Pt layer when Si reaches the surface of the Pt. A breach in the Pt reaction barrier layer allows the diffusion of Si into the

ferroelectric film and also allows the diffusion of Pb into the underlying Si substrates.⁷

Because of the difficulties encountered with bare-Si and Pt-coated Si substrates, many groups utilize substrates based on the Pt/Ti/SiO₂/Si multilayer structure.⁸⁻¹¹ This multilayer substrate provides an excellent electrode and reaction barrier layer for Pb-based perovskites, but as is shown in this paper, its applicability has a limited temperature range, and the thickness and the quality of each layer are fundamental to the high temperature stability of the structure.

This paper provides a brief review of the reactions involved with this substrate system and presents a combination of electron microscopy, Auger electron spectroscopy, and spectroscopic ellipsometry to characterize the multilayer substrates in an as-grown state and after exposure to annealing. Spectroscopic ellipsometry is a technique used for nondestructively depth profiling samples. Fundamentally, the method involves measuring the change in the polarization state of a light beam when it is reflected from a sample surface. This polarization state change depends on the depth profile of the dielectric function for the material. Thus, by collecting data at many wavelengths, it is possible to extract information on the sample by computer modeling the composition profile of the sample. Typically, the resulting depth resolution is in the angstrom range. Consequently, it complements the other characterization techniques utilized. In this paper, particular emphasis is placed on comparing the stability of the electrode structure when

^{a)}Present address: Laboratoire de Céramique, Ecole Polytechnique Fédérale de Lausanne, Lausanne, Switzerland, CH-1015.

it is annealed with and without a ferroelectric coating. The combination of results has provided a knowledge of the reactions and limitations of Pt/Ti/SiO₂/Si substrates during annealing when the Pt layer is exposed to oxidizing atmospheres and when it is covered with Pb-based ferroelectric films.

II. EXPERIMENTAL PROCEDURE

Wafers of [111] oriented Si with a 1 μm surface layer of thermally grown SiO₂ were coated with 20 nm Ti and 200 nm Pt by rf magnetron sputtering from a Ti and Pt target, respectively. Both metals were sputtered in an Ar atmosphere at a pressure of 1.6 Pa with an applied rf power of 280 W. The temperature of the substrates remained below 50 °C during the deposition process. The substrates were found to be $\langle 111 \rangle$ textured by x-ray diffraction (Pad V diffractometer, Scintag, Santa Clara, CA). For the SEM measurements, samples were annealed in a quartz tube furnace in flowing oxygen with a flow rate of 0.5 l/min.

Micrographs were obtained using a JFM 890 Field Emission Gun Scanning Electron Microscope (JEOL Ltd., Japan) with an acceleration voltage of 15 kV. Transmission images were obtained using a 2000 FX analytical electron microscope (JEOL Ltd., Japan) and a 4000 EX ultrahigh resolution transmission electron microscope (JEOL Ltd., Japan). The 2000 FX microscope was used in the scanning transmission configuration to obtain a 10 nm beam diameter for collection of energy dispersive spectra.

The substrates were also examined before and during *in situ* annealing with a rotating analyzer spectroscopic ellipsometer equipped with a heating chamber.¹² This instrument is capable of an accuracy of 0.03° and 0.01° in the ellipsometric parameters Δ and Ψ . Measurements were taken at 5 nm increments over the spectral range of 300–800 nm, using an incidence angle of 70 °C. Below 350 °C, data were collected at the annealing temperature. For higher annealing temperatures, the sample was held at the desired temperature for 0.5 h and then cooled below 450 °C to eliminate errors associated with glow from the furnace. The heating rate used throughout was 2 °C/min.

The raw ellipsometric spectra were analyzed using reference dielectric functions for each material. Multi-layer structures were modeled assuming that the layers were isotropic and parallel to the surface of the film. Bruggeman effective medium averaging was employed to calculate the dielectric properties of two or three phase mixtures. Output from the fitting program included values for the “best-fit” parameters, 90% confidence limits for each variable, a correlation coefficient matrix describing the inter-relatedness between variables, the unbiased estimator, σ ,¹³ of the goodness of fit, and

calculated Δ and Ψ spectra for the final model. All of these factors were examined to determine the best-fit model.

Finally, Auger spectroscopic measurements were taken on a Perkin-Elmer PHI660 scanning Auger microprobe. Depth profiling was accomplished with 4 kV Ar⁺ ion beam to sputter-etch the surface. A 5 kV electron beam was used as the probe.

Ferroelectric lead lanthanum titanate (PLT) and lead zirconate titanate (PZT) films were deposited on these substrates by multi-ion-beam reactive sputtering (MIBERS) and sol-gel spin-coating methods. Details on the ferroelectric film deposition have been given elsewhere.¹⁴

III. RESULTS AND DISCUSSION

A. Substrate microstructure development—Annealing with ferroelectric overlayer

The as-grown Pt layer of the substrate exhibits a columnar structure, typical of sputter deposited films,¹⁵ consisting of 20 nm diameter columns (Fig. 1). X-ray and electron diffraction indicate that the columns have a $\langle 111 \rangle$ texture perpendicular to the substrate surface.

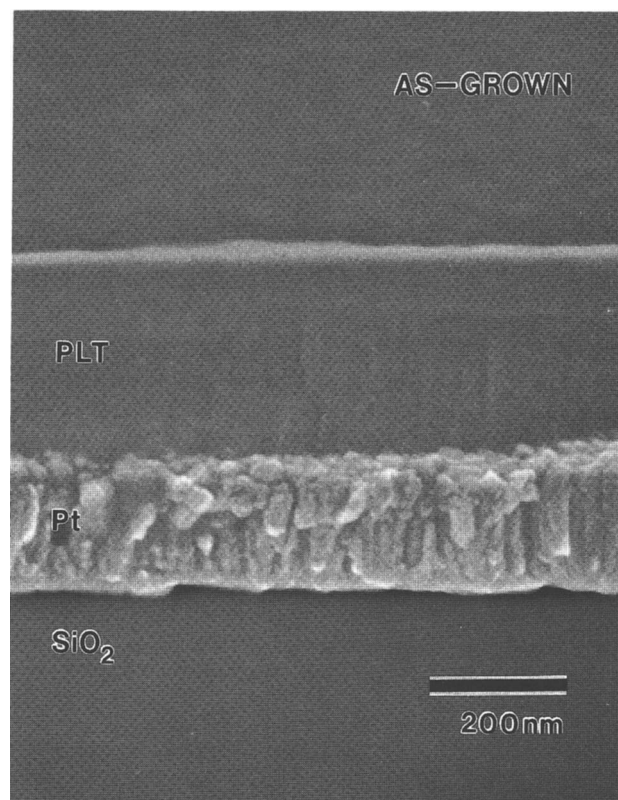


FIG. 1. Fracture cross-section SEM image of an as-deposited Pt film with an as-deposited MIBERS lead lanthanum titanate film on the surface.¹³ The Pt layer consists of 20 nm columnar grains with a $\langle 111 \rangle$ texture perpendicular to the plane of the film.

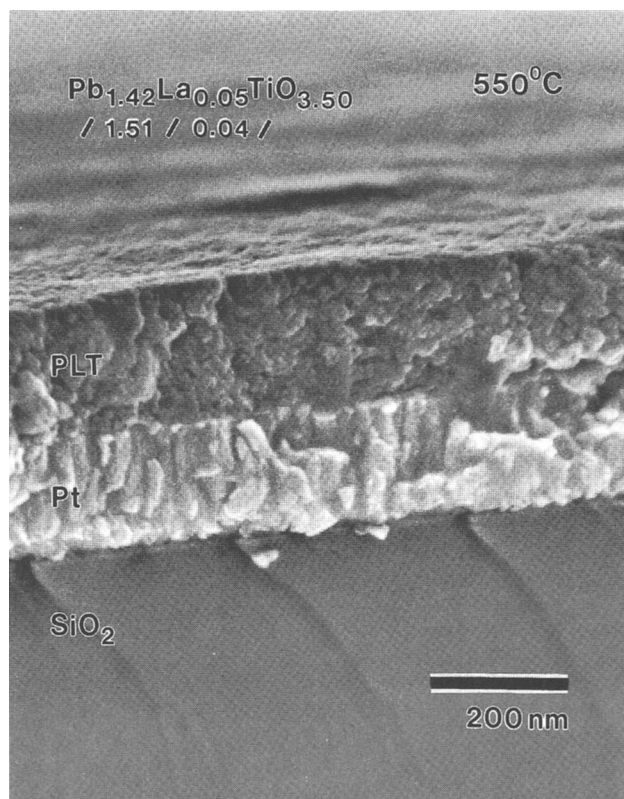


FIG. 2. Fracture cross-section SEM image of a PLT coated Pt film annealed at 550 °C for 20 min in flowing O₂. The PLT film was deposited by MIBERS.

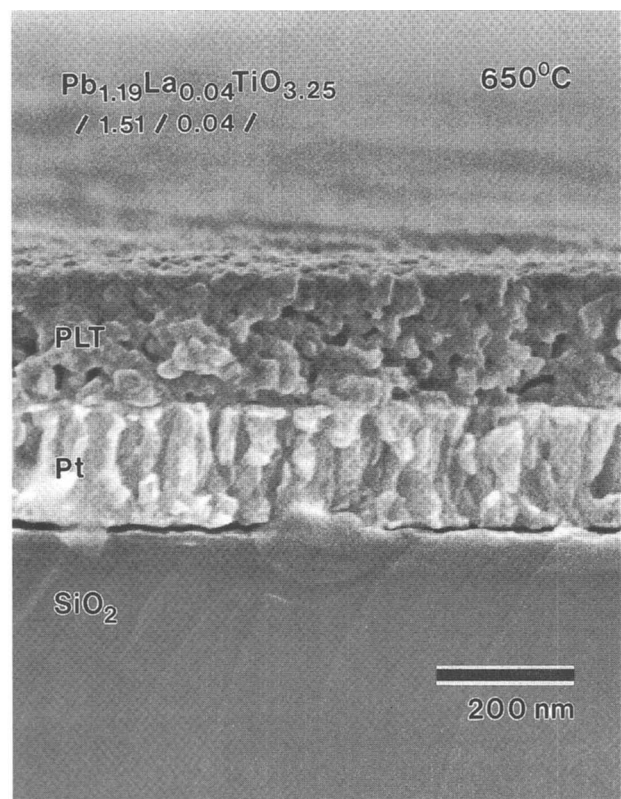


FIG. 3. Fracture cross-section SEM image of a PLT coated Pt film annealed at 650 °C for 20 min in flowing O₂. The PLT film was deposited by MIBERS.

The appearance of the microstructure of the Pt film after annealing is dependent on whether the Pt surface is exposed to the annealing atmosphere or whether another thin film material is covering the Pt. For samples where the Pt was coated with 200 nm of lead lanthanum titanate, the Pt layer could be annealed at temperatures as high as 650 °C without a significant change in the columnar structure. Coated Pt films annealed at 550 °C (Fig. 2) exhibited very little change when compared with the as-deposited films. Annealing at 650 °C for 20 min maintained the columnar structure although the film densified and grain growth mechanisms caused the diameter of the columns to increase to 50 nm (Fig. 3). Annealing at 750 °C for 20 min resulted in a loss of the Pt columnar structure due to extensive grain growth (Fig. 4).

An EDS composition profile of a cross-section sample annealed at 650 °C for 20 min (Fig. 5) showed the diffusion behavior of the various layers during annealing. No Ti was observed in the SiO₂ layer, which indicated that Ti did not react with the SiO₂; this is anticipated due to the insolubility of TiO₂ in SiO₂.¹⁶ Moving into the Pt from the SiO₂/Ti/Pt interface, the Ti signal decreased and no Ti was detected at distances greater than 100 nm from the interface. This profile suggests that the Ti

diffused into the Pt and formed a Pt_xTi_{1-x} alloy with a graded composition.¹⁷ Only Pt was observed in the top 100 nm of the Pt layer, confirming that none of the elements of the PLT film diffused into the Pt. A surface roughness of approximately 20 nm for the Pt at the Pt/PLT interface is estimated from Fig. 5. The figure also shows clearly that the Pt columns are single grains, rather than polycrystals.

Pt/Ti/SiO₂/Si substrates capped with ferroelectric films were also investigated by spectroscopic ellipsometry before and after the films were annealed to crystallize the ferroelectric. It was found that for both sol-gel and MIBERS PZT films deposited at room temperature, the film-substrate system could be well-modeled using the dielectric function for the unannealed substrate and a Sellmeier oscillator for the amorphous films. Several classes of behavior were observed when the films were subsequently heated to crystallize the ferroelectric. Films annealed at 600 °C for under 20 min did not show significant changes in the substrate optical properties, even though the PZT films were well-crystallized. In contrast, many PZT films annealed in a conventional furnace for 650 °C for an hour or more showed unreasonably high refractive indices for the perovskite (~0.1 too high over the entire spectral range) when it was assumed that the

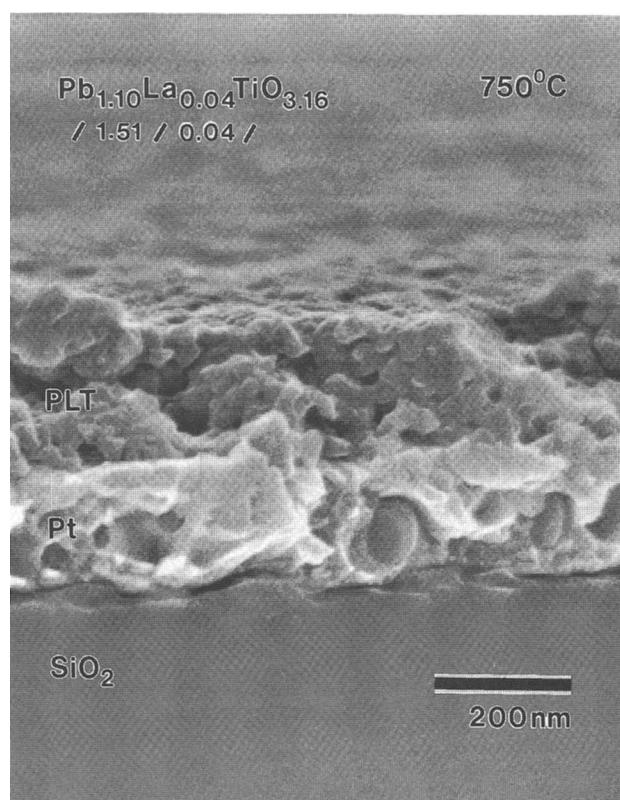


FIG. 4. Fracture cross-section SEM image of a PLT coated Pt film annealed at 750 °C for 20 min in flowing O₂. The PLT film was deposited by MIBERS.

substrate remained unchanged during the heat treatment. Such large refractive indices were not observed in PZT films fired under the same conditions that were prepared on sapphire substrates. Consequently, the anomalous refractive indices were attributed to changes occurring in the Pt/Ti/SiO₂/Si effective dielectric function (perhaps due to changes in the substrate surface microstructure or composition) upon annealing. In many cases, the modeled PZT film refractive index could be reduced to reasonable values by fitting the data with a model including a roughened PZT film/substrate interface. It is also possible that part of the observed change may be due to migration of Ti to the substrate surface, where it would presumably oxidize on reaching the Pt surface. It was not possible to determine whether this occurred solely on the basis of the spectroscopic ellipsometry data.

In general, the fact that the substrate effective dielectric function is not well defined limits the accuracy to which the refractive index of insulating films on Pt/Ti/SiO₂/Si substrates can be determined. It is interesting to note, however, that the modeled depth profiles for the film modeled with and without changes in the substrate are largely the same. Consequently, it should be possible to use spectroscopic ellipsometry to interrogate the microstructure of films on Pt/Ti/SiO₂/Si substrates.

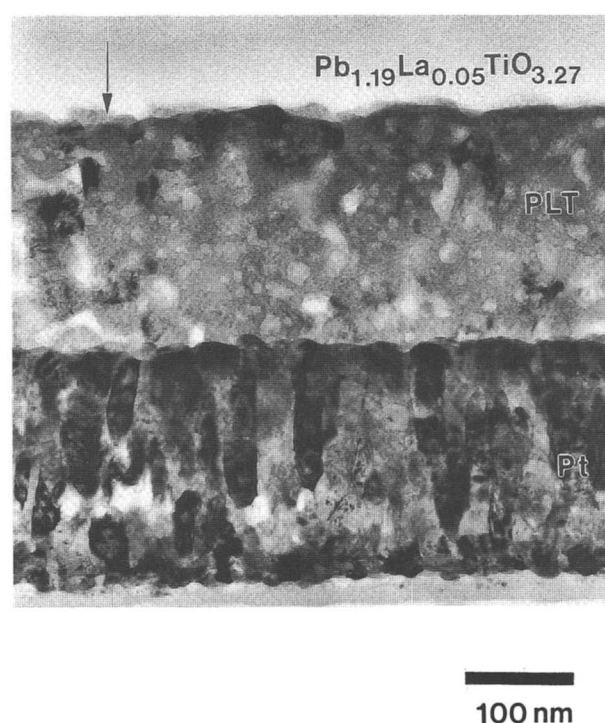


FIG. 5. Bright-field TEM image of a PLT coated Pt film annealed at 650 °C for 20 min. The PLT film was deposited by MIBERS.

The absolute value of the refractive index (and hence any density value derived from the optical properties), however, will contain some uncertainty.

B. Substrate microstructure development—Annealing Pt film with exposed surface

Surface images of as-received substrates are compared with uncoated Pt/Ti/SiO₂/Si substrates annealed at 650 °C for 20 min in Figs. 6–8. A high magnification image of the as-received Pt surface (Fig. 6) reveals 30-nm column diameters at the surface. During annealing, the column diameter grows to approximately 50 nm, the grain surfaces become rounded, and the grain boundaries more defined [Fig. 6(b)]. As the magnification is decreased, it is found that for a 3 × 4 μm area, the as-received substrates (Fig. 7) have a uniform surface. In contrast, two types of defects are observed on the annealed substrates [Fig. 7(b)]. The defects labeled A are beads of Pt approximately 150 nm in diameter. Since Pt is known to have high surface mobility at the annealing temperature in oxidizing atmospheres, it is likely that the Pt beads are formed by Ostwald ripening on the Pt surface.^{18,19} The dark region labeled B exhibits the Pt

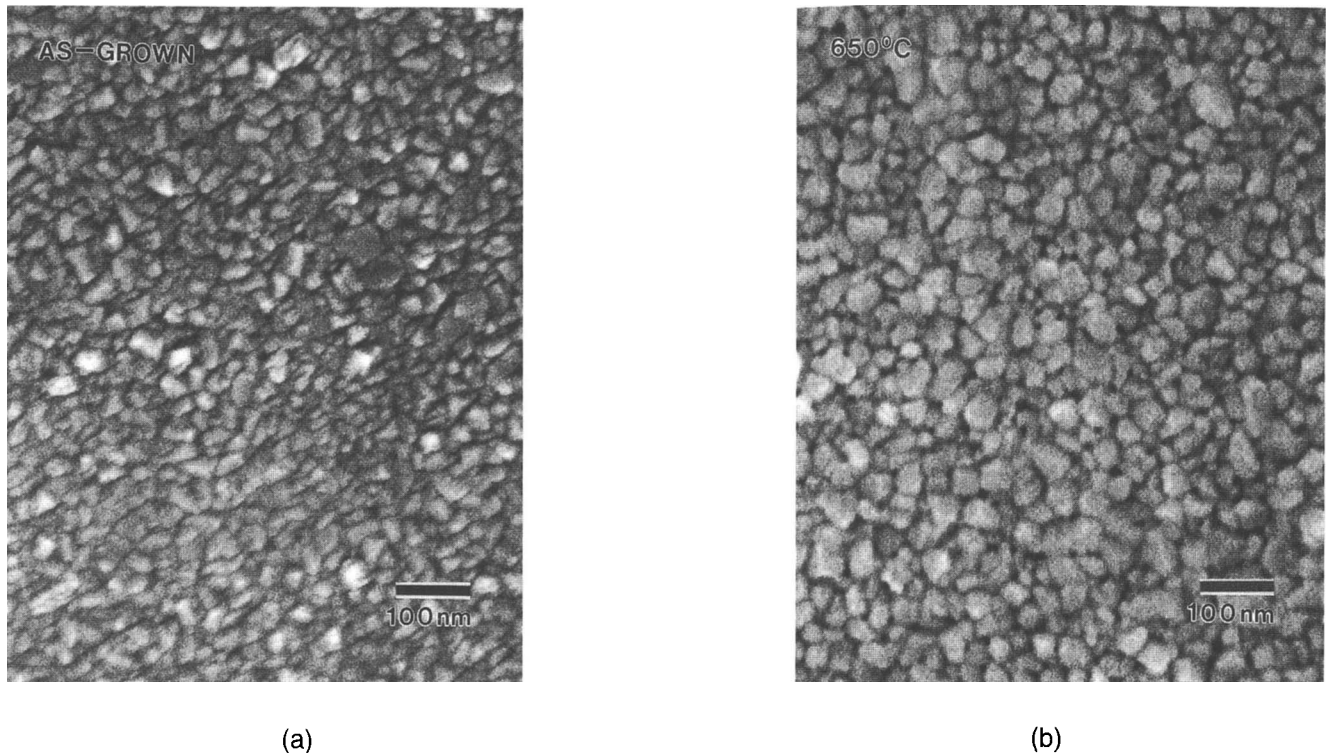


FIG. 6. SEM surface image of (a) the as-grown Pt/Ti/SiO₂/Si substrate and (b) a Pt/Ti/SiO₂/Si substrate after annealing at 650 °C for 20 min in flowing O₂.

grain structure, but the dark appearance indicates that the region is lower in density than the surrounding material. Diffusion of Si or Ti to the surface of the Pt, resulting in the formation of Pt alloys, a silicon oxide, or a titanium oxide, may be the source of these defects.²⁰ The B-type defects range in size from 0.1 to 1 μm .

Larger area micrographs (for a $60 \times 70 \mu\text{m}$ area) show the distribution of defects for both as-received and annealed substrates. Over this area, the as-received substrates exhibit a low number of defects that are probably due to dust particles collected during preparation and handling. The micrograph of the annealed substrate exhibits a large number of the A-type, Pt bead defects (white dots), and a small number of B-type defects (black circles). The density of these defects can be estimated from Fig. 8. It was found, however, that the number of each type of annealing-induced defect varied significantly from wafer to wafer. Many wafers did not contain the B-type defect but contained large numbers of A-type defects after annealing.

Neither of the annealing-induced defects has been observed in SEM or TEM cross-section images when a ferroelectric film is present during the annealing process. Because the Pt beads are believed to result from surface diffusion, it is likely that a thick oxide film limits surface diffusion of the Pt and therefore minimizes formation of beads. The formation of the less common B-type defects

may also be altered with the addition of the surface oxide film due to a change in the availability of oxygen for reaction with Ti.²⁰

In order to probe changes in the electrode surface microstructure and composition during annealing, spectroscopic ellipsometry was used to follow *in situ* the annealing of a substrate without a ferroelectric surface film. In this experiment, spectroscopic ellipsometry data were collected in 50 °C temperature intervals from room temperature to 600 °C. Measurements and annealing were performed in air.

Figure 9 shows the experimental Δ and Ψ spectra as a function of the substrate annealing temperature. Data taken prior to heating could be modeled well as a layer of roughened platinum on platinum (i.e., the top surface roughness layer consisted of a $1.8 \pm 0.2 \text{ nm}$ thick layer composed of $67 \pm 3 \text{ vol.}\%$ Pt and $33 \pm 3 \text{ vol.}\%$ air). As the penetration depth of visible light in platinum is on the order of a few hundred angstroms, it was not possible to characterize any of the layers buried deeper in the substrate. At comparatively modest temperatures ($\sim 250 \text{ }^\circ\text{C}$), the Δ and Ψ spectra altered somewhat. This is most likely due to small changes in the Pt microstructure.

Above 500 °C, however, substantial changes in the ellipsometric spectra occur as is evident from Fig. 9. Moreover, by 550 °C, the spectra for Δ and Ψ have

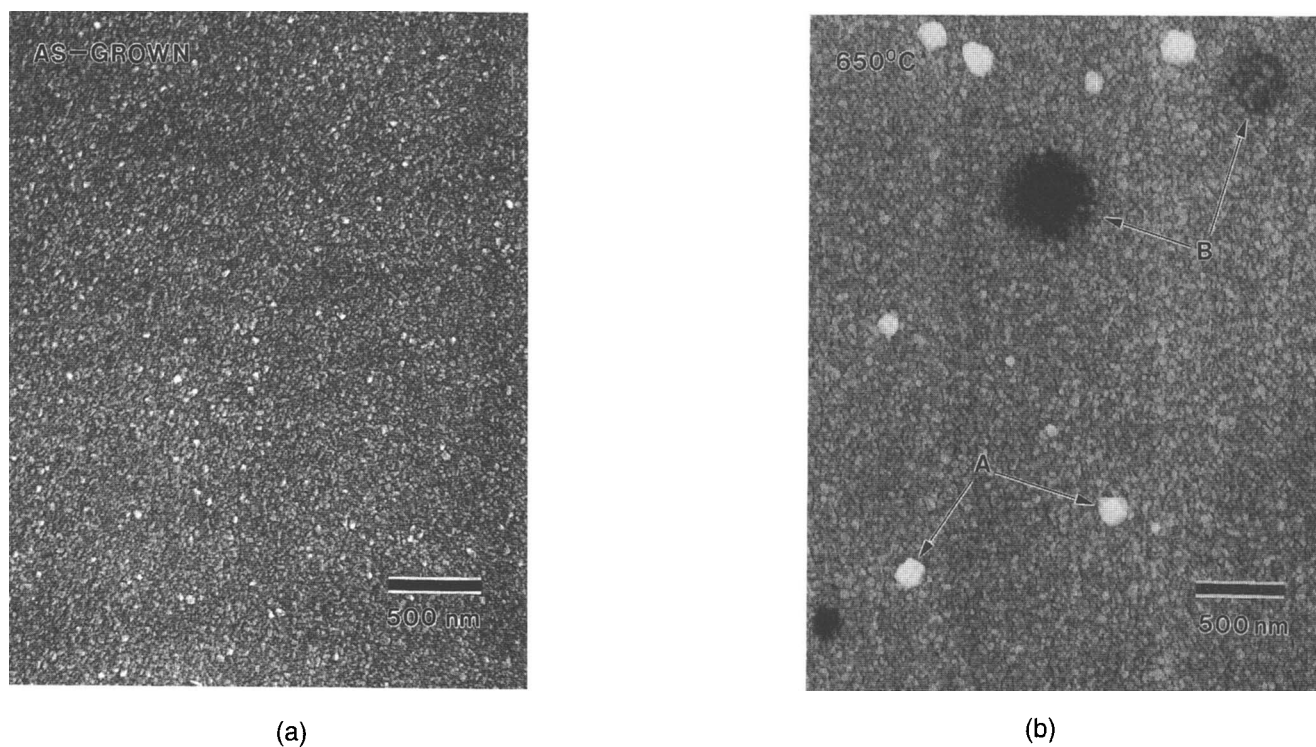


FIG. 7. SEM surface image (a) of the as-grown Pt/Ti/SiO₂/Si substrate showing the uniformity of a $3 \times 4 \mu\text{m}$ area and (b) showing Pt bead defects (A) and low density regions (B) that appear after annealing the Pt/Ti/SiO₂/Si substrates in flowing O₂ at 650 °C for 20 min.

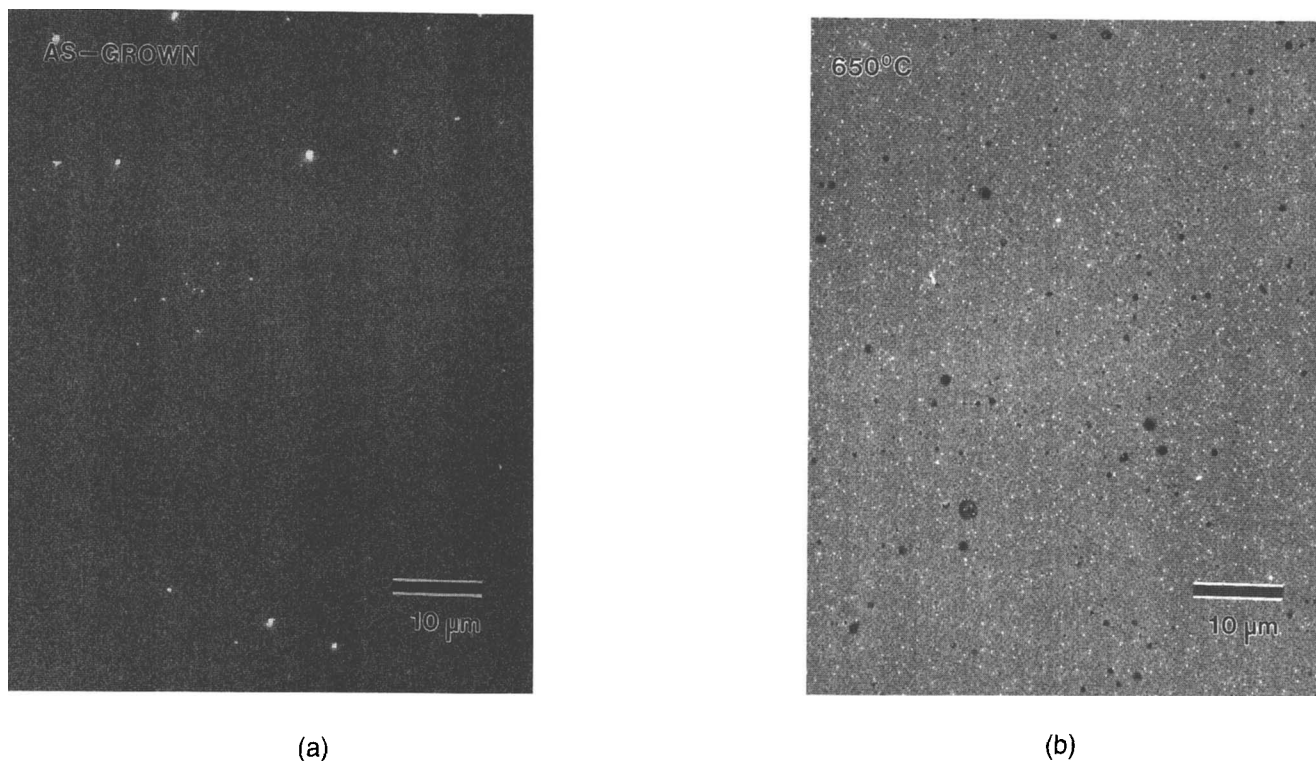


FIG. 8. SEM surface image of a $60 \times 70 \mu\text{m}$ area on (a) an as-grown Pt/Ti/SiO₂/Si substrate and (b) a Pt/Ti/SiO₂/Si substrate annealed in flowing O₂ at 650 °C for 20 min. The image shows the distributions of the two types of defects formed when the substrates are annealed without a surface coating.

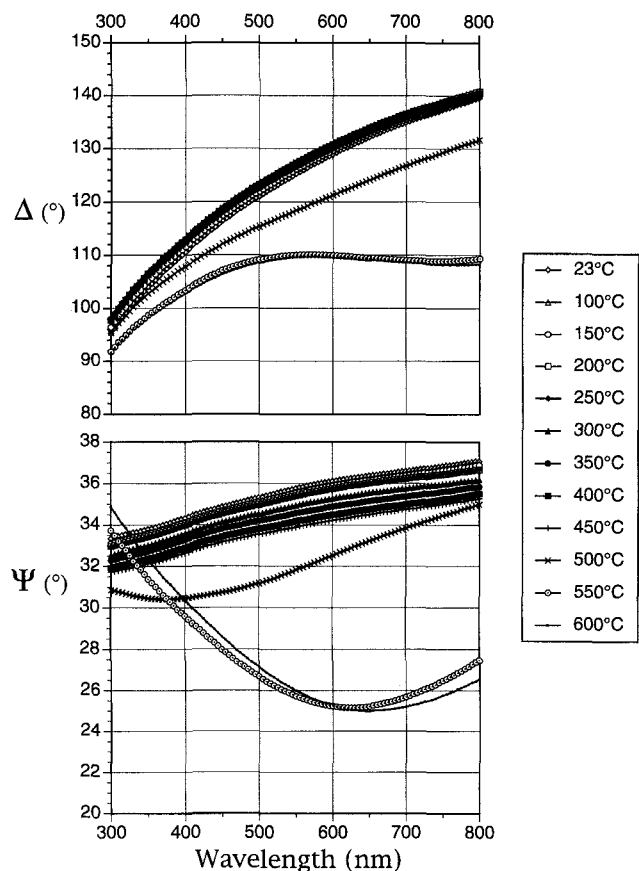


FIG. 9. Raw spectroscopic ellipsometry data for a Pt/Ti/SiO₂/Si substrate during *in situ* annealing.

both developed markedly different curvatures, implying the formation of interference oscillations associated with a transparent film on the platinum surface. The existence of these features was confirmed on a sample heated *in situ* using the same temperature profile. Modeling of these data was extremely difficult, probably due to the extensive hillocking of the Pt surface. Attempts to model the data with combinations of Pt, PtO, and air were unsuccessful. Instead, the top surface was better modeled with a thin layer of a dielectric material.

It was conjectured that the transparent overlayer seen in the optical studies could be attributed to migration of one of the oxidizable components of the substrate through the Pt barrier layer. This result is consistent with the EDS data which suggested the migration of Ti through the Pt electrode layer. For the lengthy annealing process utilized in the *in situ* annealing on the spectroscopic ellipsometer, Ti apparently diffused through the Pt to the surface and oxidized. To confirm that the layer was in fact due to TiO₂, Auger electron spectroscopy was used to depth profile the sample. As can be seen in Fig. 10, the unannealed substrate showed a fairly abrupt interface between the Pt and the Ti [the

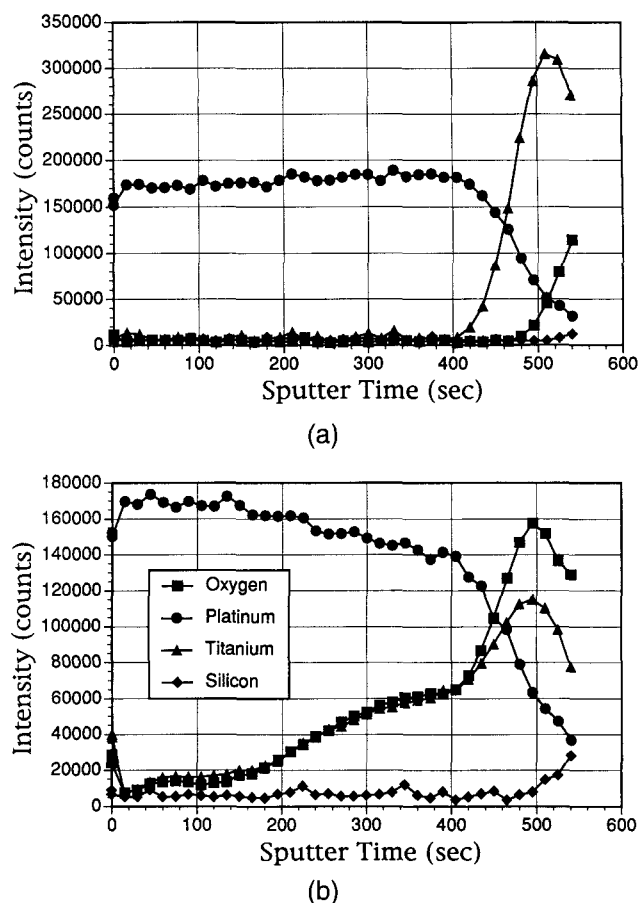


FIG. 10. Auger electron spectroscopy depth profile of (a) an unannealed Pt/Ti/SiO₂/Si substrate and (b) the Pt/Ti/SiO₂/Si substrate that underwent *in situ* annealing in the spectroscopic ellipsometer.

breadth of the transition region in Fig. 10(a) is probably associated with knock-in rather than true intermixing]. Figure 10(b), which shows the results for a sample annealed under the same conditions as those used in the spectroscopic ellipsometry analysis, indicates that Ti and O have diffused through the thickness of the Pt layer. No penetration of Si into the Pt layer was observed. Thus, it is clear that during heat-treatment significant microstructural and chemical changes can occur in Pt-coated Si substrates with a Ti adhesion layer. These results on Ti migration are consistent with recent reports by Sreenivas *et al.*¹¹ and Bruchhaus *et al.*⁹ for thick Ti barrier layers in Pt/Ti/SiO₂/Si substrates.

It is also important to note that the appearance of the transparent surface film in spectroscopic ellipsometry measurements is strongly dependent on the annealing profile. Thus, substrates that were heated to 600 °C and held for 20 min did not show such a change in curvature, while films heated to the same maximum temperature, but which were exposed to prolonged heat treatments at lower temperatures, did.

Diffusion of Ti through the substrate can have some important consequences in terms of the observed electri-

cal properties of ferroelectric films on these substrates. In particular, if the diffusion is allowed to proceed to the point that a layer of a TiO₂ forms on the surface, then the observed electrical properties will be modulated by the presence of the low dielectric constant TiO₂ layer between the ferroelectric and the bottom electrode. This would result in a decrease in the observed dielectric constant and an increase in the coercive field of the ferroelectric film. This type of deterioration in properties is expected to be especially severe when the substrate is held at temperatures in excess of ~500 °C prior to deposition of the ferroelectric film.

IV. CONCLUSIONS

Pt/Ti/SiO₂/Si substrates undergo chemical and microstructural changes during annealing at temperatures typically utilized for the preparation of ferroelectric thin films. These include grain growth of the original columnar microstructure, the formation of defects, and the migration of Ti through the Pt layer. Some of these changes are retarded when the surface of the Pt is coated with a ferroelectric overlayer. The movement of Ti may be deleterious to the observed electrical properties of a thin film deposited on such substrates, as it may act as an insulating barrier layer between the film and the electrode.

ACKNOWLEDGMENTS

The authors would like to thank Karen More for her part in the TEM work. This work was partially sponsored by the United States Department of Energy, Assistant Secretary for Conservation and Renewable Energy, Office of Transportation Technologies, as part of the High Temperature Materials Laboratory User Program, under Contract DE-AC05-84OR21400 managed by Martin Marietta Energy Systems, Inc. Travel expenses

to Oak Ridge National Laboratory were provided by Oak Ridge Associated Universities.

REFERENCES

1. R. S. Roth, and L. P. Cook, *Phase Diagrams for Ceramists* (The American Society, Westerville, OH, 1981), Vol. IV.
2. S. K. Dey and R. Zuleeg, *Ferroelectrics* **108**, 37 (1990).
3. L. D. Madsen and L. Weaver, *J. Electron. Mater.* **21** (1), 93 (1992).
4. R. A. Roy and K. F. Etzold, *J. Mater. Res.* **7**, 1455 (1992).
5. R. Pretorius and A. P. Botha, *Thin Solid Films* **79**, 61 (1981).
6. L. S. Hung and J. W. Mayer, *J. Appl. Phys.* **60** (3), 1002 (1986).
7. G. Fox and S. B. Krupanidhi, unpublished work.
8. J. O. Olowolafe, R. E. Jones, A. C. Campbell, P. D. Maniar, R. I. Hedge, and C. J. Mogab, in *Ferroelectric Thin Films II*, edited by A. I. Kingon, E. R. Myers, and B. Tuttle (Mater. Res. Soc. Symp. Proc. **243**, Pittsburgh, PA, 1992), p. 355.
9. R. Bruchhaus, D. Pitzer, O. Eibl, U. Scheithaurer, and W. Hoesler, in *Ferroelectric Thin Films II*, edited by A. I. Kingon, E. R. Myers, and B. Tuttle (Mater. Res. Soc. Symp. Proc. **243**, Pittsburgh, PA, 1992), p. 123.
10. I. Kondo, T. Yoneyama, O. Takenaka, and A. Kinbara, *J. Vac. Sci. Technol. A*, **10** (6), 3456 (1992).
11. K. Sreenivas, I. Reaney, T. Maeder, N. Setter, C. Jagadish, and R. G. Elliman, *J. Appl. Phys.* **75** (1), (1994).
12. S. Trolier-McKinstry, H. Hu, S. Krupanidhi, P. Chindaudom, K. Vedam, and R. E. Newnham, *Thin Solid Films* **230**, 15 (1993).
13. D. E. Aspnes and J. B. Theeten, *Phys. Rev. Lett.* **43**, 1046 (1979).
14. G. R. Fox, S. B. Krupanidhi, K. L. More, and L. F. Allard, *J. Mater. Res.* **7**, 3039 (1992); S. B. Krupanidhi, H. Hu, and V. Kumar, *J. Appl. Phys.* **21**, 376 (1992); J. Chen, K. R. Udayakumar, K. G. Brooks, and L. E. Cross, *J. Appl. Phys.* **71**, 4465 (1992).
15. J. A. Thornton, *Annu. Rev. Mater. Sci.* **7**, 239 (1977).
16. E. M. Levin, C. R. Robbins, and H. F. McMurdie, *Phase Diagrams for Ceramists*, 3rd ed. (The American Ceramic Society, Westerville, OH, 1974), p. 69.
17. T. C. Tisone and J. Drobek, *J. Vac. Sci. Technol.* **9** (1), 271 (1971).
18. R. A. Roy, K. F. Etzold, and J. J. Cuomo, in *Ferroelectric Thin Films*, edited by E. R. Myers and A. I. Kingon (Mater. Res. Soc. Symp. Proc. **200**, Pittsburgh, PA, 1990), p. 141.
19. Y. F. Chu and E. Ruckenstein, *Surf. Sci.* **67**, 517 (1977).
20. Y. M. Sun, D. N. Belton, and J. M. White, *J. Phys. Chem.* **90**, 5178 (1986).